27

Rapid #: -2883230

Ariel IP: 150.135.238.50

Status	Rapid Code	Branch Name	Start Date
Pending	IWA	Main Library	10/20/2009 5:43:46 PM

CALL #: QH505 A1 B52
LOCATION: IWA :: Main Library :: gen

TYPE: Article CC:CCL
JOURNAL TITLE: Biorheology
USER JOURNAL TITLE: Biorheology (Oxford)
IWA CATALOG TITLE: Biorheology
ARTICLE TITLE: The flow and dispersion of water in the vascular network of dicotyledonous leaves
ARTICLE AUTHOR: Jeje, A
VOLUME: 22
ISSUE: 4
MONTH:
YEAR: 1985
PAGES: 285-302 KMS.
ISSN: 0006-355X
OCLC #:
CROSS REFERENCE ID: 702647
VERIFIED:

BORROWER: AZU :: Main Library
PATRON: Blonder, Benjamin W

PATRON ID:
PATRON ADDRESS:
PATRON PHONE:
PATRON FAX:
PATRON E-MAIL:
PATRON DEPT:
PATRON STATUS:
PATRON NOTES: SS-google

System Date/Time: 10/21/2009 7:38:46 AM MST

3. MATRAI, A., ERNST, E., FLUTE, P.T. and DORMANDY, J.A. Blood filterability in peripheral vascular disease - red cell deformability or cell sticking? Clinical Haemorheology, in press.

4. HANSS, M. Erythrocyte filterability measurement by the initial flow rate method. Biorheology, 20, 199-211, 1983.

5. GREGERSEN, M.I., BRYANT, G.A., HAMMERLE, W., USAMI, A. and CHIEN, S. Flow characteristics of human erythrocytes through polycarbonate sieves. Science, 157, 825-827, 1967.

6. LUCAS, G.S., CALDWELL, N.M., KENNY, M.W., MEAKIN, M., AILLAUD, M.F., BILLEREY, M., JUHAN-VAGUE, I. and STUART, J. Effect of calcium-chelating and non-chelating anticoagulants on erythrocyte and leucocyte filterability. Clinical Haemorheology, 31. 451-467, 1983.

7. KOUTSOURIS, D., HANSS, M. and SKALAK, R. Determination of erythrocytes transit times through a 5 u "Nucleopore" filter. Biorheology 20, 770-788, 1983.

8. SKALAK, R., IMPELLUSO, E., SCHMALZER, E. and CHIEN, S. Theoretical modelling of filtration of blood cells suspensions. Biorheology, 20, 41-56, 1983.

BIORHEOLOGY, 22; 285-302, 1985
0006-355X $3.00 + .00 Printed in the USA.

THE FLOW AND DISPERSION OF WATER IN THE VASCULAR NETWORK OF DICOTYLEDONOUS LEAVES

AYODEJI A. JEJE
The University of Calgary, Alberta, Canada T2N 1N4

(Received 12.2.1985; in revised form 4.4.1985
Accepted 11.4.1985 by Editor S. Oka)

ABSTRACT

The relationships between the geometric characteristics of, the local flow rates of xylem sap in, and relative pressures in the reticulate anastomosing vascular network of dicotyledonous leaves of Populus Balsamifera L.are reported. The conducting channels of cellulosic microcapillaries are covered by sheaths of chloroplast free cells through the walls of which water withdrawn from vascular bundles percolates to reach evaporation sites. Along the mid-rib and branch generations, the population and cross-section areas of the microcapillaries decrease with distance but not in a monotonic manner. Lateral withdrawal rates from the veins were highest at the base of the leaf lamina. More than 50% of the inlet stream had dispersed out of the conduits within the first 25% of the leaf lamina area from the petiole junction. Absolute values of pressure gradients generally decreased in the apical direction along the vein.

INTRODUCTION

The veins (fibro-vascular bundles) of leaves of terrestrial plants serve two primary functions. One is to provide a two-dimensional structural framework for the support of mesophyll parenchyma cells, that is, the cells containing chloroplasts within a flat, thin blade enclosed by the epidermis. The second function which is of current interest involves the irrigation of the leaf with water. Water entering the petiole (leaf stalk) is distributed via the veins to the cells to sustain turgidity, translocation of assimilates in the phloem out of the leaf, and biochemical reactions in the cytoplasms. Most of the water, however, percolates the extrafascicular

Fascicular flow, vascular network, dicotyledonous leaves

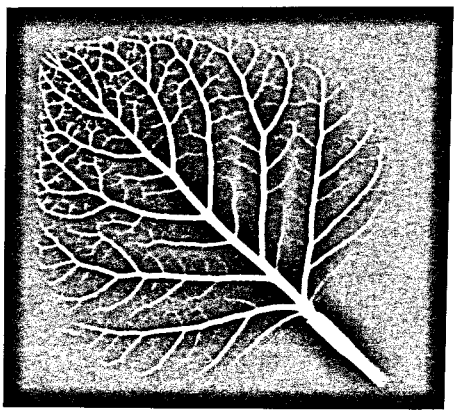

FIG. 1

The vascular network of a leaf of a horticultural variant of Populus Balsamifera L.

apoplast, i.e. force spaces of the cell walls (1,2), and is evaporated at cell surfaces exposed to the intercellular mesophyll gas space.

The veins in the leaves of dicotyledons normally form reticulate anastomosing networks with smaller veins diverging laterally from the larger ones (Figure 1). Typically, the veins comprise of cellulosic microcapillaries, xylem vessels and tracheids, surrounded by layers of chloroplast-free parenchyma and collenchyma (fiber) cells termed sheaths. The large veins (tracheal elements and sheath) form ridges on the abaxial surface of the leaf. The fibro-vascular bundles in minor venations, i.e. after the first or second generation branches are entirely enclosed by the epidermis and reflect a modified geometrical structure of the sheath. Some of the sheath cells appear as plates which are oriented normal to the veins and are layered to extend and touch both epidermis (3). Such oriented parenchyma cells are called bundle-sheath extensions and they are involved in the transport of water from the tracheal elements primarily to the inner surfaces of epidermal cells (4,5). Generations of branches successively enclose smaller polygonal leaf areas and the veins may ultimately terminate with one or more unsheathed tracheids radiating freely into the smallest transverse sub-division of the leaf, the areole (6). Some areoles may not have free vein endings, that is, such areoles are subtended by apparently closed loops of vessel elements or tracheids which may have sheaths on most sides of the polygon (7). The extent of sheathing along the length of all veins and the frequency of bundle-sheath extensions have been reported correlated to the density of the vascular network. If most of the veins are covered by the sheath, and bundle-sheath extensions are present in most minor veins, the vascular network is less elaborate (8,9).

The distribution of water in a leaf may be qualitatively described as follows. Water which enters the leaf is divided into the major veins where, as it is convected in the tracheal elements, a fraction is withdrawn across the sheath to supply nearby cells. Since major veins typically constitute about 5% of the total length of all veins, the amount withdrawn has in general been assumed to be small. The various generations of minor veins are believed to disperse most of the water (5). Terminal tracheal elements without sheaths, when present, irrigate mainly the walls of the contiguous spongy and palisade parenchyma cells. Typically, the most remote parenchyma

cell is no further than five or six cells away from a vein or veinlet for mesomorphic plants (7).

The distribution of water into the network of major and minor veins has been investigated quantitatively in the present study. Local volumetric flow rates in the veins were determined from the velocities and the tracheal elements net cross-sectional areas at known distances from the mid-rib and along the mid-rib. Lateral rates of water loss from the conducting channels could then be evaluated. Extrafascicular transport which depend on the permeability of cell walls, the cell dimensions and organization, density of sheath extensions and the forces actuating the water dispersion has not been directly examined in this paper. Of interest is water depletion from the tracheal elements as water is convected into progressively fewer vessels along each major or minor vein. This is related to a determination of whether some areas of a leaf are more efficiently involved with transpiration than other areas. The pressure gradients associated with the observed flow rates are also of interest.

Geometrical Characteristics of Leaves of the Plant Investigated

Leaves of horticultural variant of the Balsam poplar (Populus Balsamifera Linneaus) were studied. The network of veins of a mature leaf was presented in Figure 1. There are typically 3 to 5 generations of branches. The mid-rib and the first generation branch from ridges on the abaxial surface of the leaf. Large second generation branches, form ridges while the smaller ones and the subsequent generations are totally enclosed within the upper and lower epidermis.

The veins as shown in Figure 1 do not fully reflect the detailed arrangement of the vessels through which water is convected. Vessels in the petiole (Figure 2a and b) are arranged in 3 to 5 fibro-vascular bundles of which the largest or dominant one is displaced to the abaxial side of the leaf. Parenchyma cells are in the core of each bundle and vessels are arranged in radial rows within the parenchyma cells. In small bundles, this radial arrangement is not evident i.e. when the number of vessels are few. Around the parenchyma cell core, sclerenchyma cells with thick walls are arranged in cresent forms which are sometimes connected. Large cells devoid of chloroplasts surround the bundles and occupy the space up to the epidermis. At the base of the leaf lamina, the fibro-vascular bundles are relocated (Figure 2c). Small bundles are now almost laterally positioned relative to the central bundle or fascicles. The small lateral bundles, or traces, conduct water into the first branches of the leaf network. The major bundle subdivides before or after the first branches on either side of the mid-rib (Figure 2d) in anticipation of the subsequent primary branches and the process repeats itself downstream along the mid-rib.

All the veins of the leaf of this plant have sheaths. In the leaf cross-section (Figure 2e), bundle-sheath cells are arranged normal to the leaf lamina. In the paradermal section (Figure 2f), the bundle-sheath extension cells are contiguous along the vein with up to five layers of elongated cells juxtaposed. These bundle-sheath extensions are present even at the vessel ends. In some areoles, vessel ends appear connected by the bundle-sheath entensions. Hence the water transported across the vessel walls must pass through the bundle-sheath cell walls and the walls of the sheath extensions before perfusing the walls of the spatially-diffuse spongy cells, two layers of oriented palisade parenchyma cells and the inner surfaces of the epidermal cells. The bundle-sheath extensions effectively compartmentalize the leaf laminar such that lateral diffusion of gases

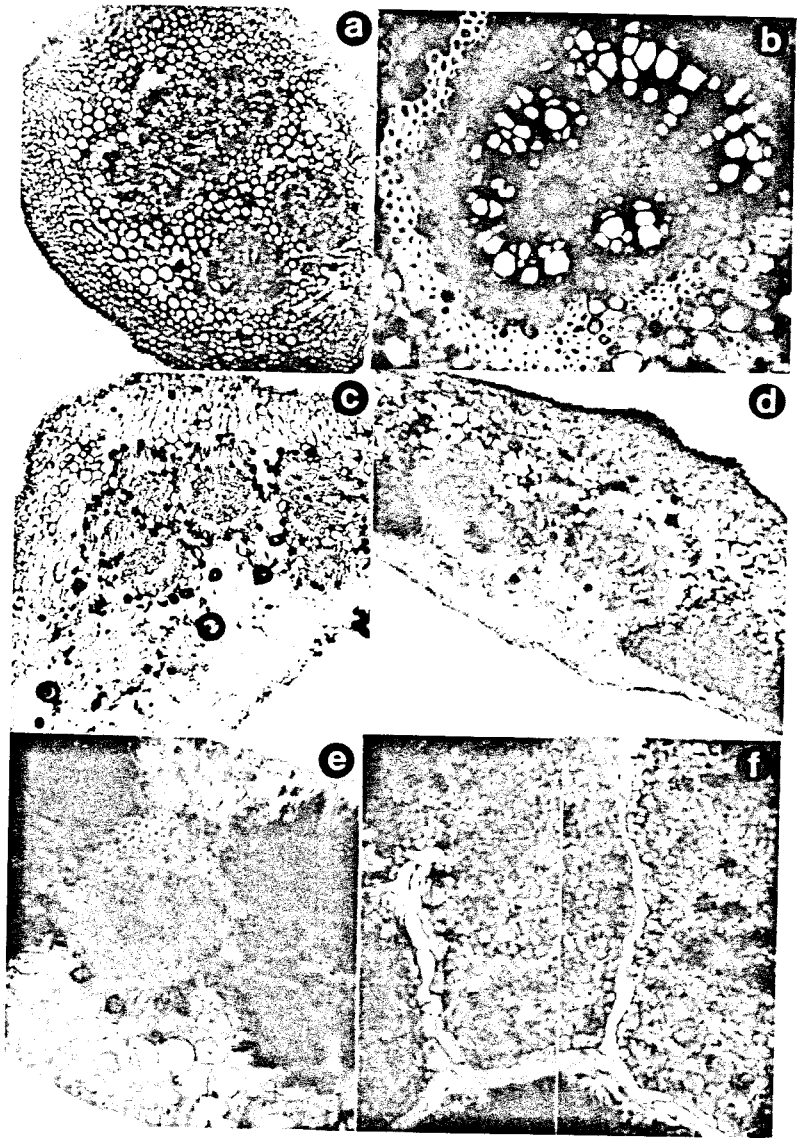

FIG. 2

The organization of vascular bundles and tracheal elements in the veins of the leaf of Balsam Poplar.
(a) Vascular bundles in the petiole cross-section, 62X
(b) Vessels in a bundle (white areas in the centre), 153X
(c) Bundles at the junction of the petiole and the leaf lamina, 62X
(d) Bundles along the mid-rib in the centre of leaf blade, 62X
(e) Cross-section of a minor vein showing the bundle sheath and extension, 153X
(f) Paradermal section of leaf showing sheath extension cells above minor veins and sections through the palisade cells, 62X

(water vapor, CO_2, O_2) within the leaf laminar between areoles would be highly restricted.

METHODS

Young leaves detached from a tree branch, with the petiole cut under water, about 1-2 weeks after buds were open, were used for the experiments. These leaves had fewer sheath and sclerenchyma cells around the vessels than fully mature leaves. The leaves were attached to calibrated uniform bore capillary tubes filled with water. Transpiration rates of the leaves were monitored over a period of about 2 hours. Both the room temperature and relative humidity were recorded. Thereafter, a leaf was rapidly transferred to another capillary tube containing a 2% w/w solution of a fluorchrome (8-hydroxy-1,3,6-pyrenetrisulphonic acid, trisodium salt) and the leaf was placed in the light path configuration shown schematically in Figure 3. During an experimental run, slugs of immersion oil covered the menisci at both ends of the capillary and prevented a direct loss of water by evaporation to the ambient from the capillary tubes. The rates of decrease in length of the liquid trapped was therefore directly related to the water uptake or transpiration rate.

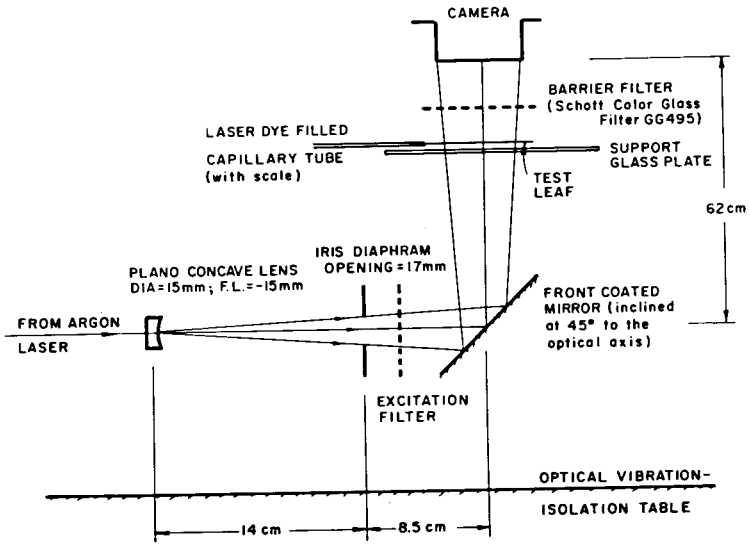

FIG. 3

A schematic diagram of the apparatus set-up.

In the optical arrangement, monochromatic blue light from an argon laser (450 - 460 nm and 200 mW power level) was expanded with a plano-concave lens , passed through an iris and then reflected using three front coated mirrors. The light traversed an excitation filter (457.9 nm), the leaf being fed the fluorchrome (test sample), 2 sharp cut-off barrier

TABLE 1

The geometrical characteristics of the mid-rib and two first generation branches of the vascular network for leaf sample #13.

	Branch	Distance From junction mm	Number of xylem vessels	Average Vessel diam. (μm)	Total Flow x-section area (μm^2)
A	Mid-rib	1.83	46	5.64	1155.9
		3.26	45	5.89	1233.2
		5.82	53	6.16	1601.0
		7.42	62	6.40	2045.0
		13.31	37	6.74	1336.0
		15.34	36	6.40	1178.0
		21.66	22	6.70	789.3
		24.58	19	6.77	692.6
		27.20	17	6.59	587.9
B	Second Branch - left side	1.66	19	6.06	547.6
		4.44	19	6.11	564.4
		6.32	18	5.89	479.6
		8.05	17	5.78	454.8
		10.86	14	4.77	258.9
		12.01	13	5.55	320.2
		13.24	12	5.43	284.0
		15.29	9	6.22	275.5
		16.77	11	5.13	231.4
		18.40	8	5.04	165.8
		20.61	8	5.06	165.7
		22.57	8	5.43	189.0
C	Second Branch - right side	1.53	25	7.26	1052.9
		4.19	19	7.29	799.1
		6.37	17	7.38	748.2
		10.18	12	7.72	564.9
		11.76	11	7.85	537.0
		14.89	11	7.75	526.6
		16.28	13	6.05	375.9
		17.43	11	6.43	360.9
		18.58	9	5.61	225.5
		21.39	8	5.99	226.5

filters (with a transmittance < 10^{-3} at light wavelengths ≦ 480 nm and > 0.9 at 515 nm) before entering the camera optics. The laser light intensity was sufficiently weak that in the course of a run no temperature changes were detected around the leaf.

Before the fluorchrome entered the leaf lamina, the veins were not visible through the camera. As the fluorchrome transversed the vessels, it absorbed the incident beam at 454 nm (optimum) and fluoresced at 515 nm. Since the conducting channels were embedded in clear (non-pigmented) cells in the direction of the light path, the penetration of the dye could be monitored as a function of time in the vascular network and recorded on film.

During and for about 30 minutes after the dye penetration period, the rate of transpiration by the entire leaf was continuously monitored. After the experiment, the leaf was cleared of chlorophyll by standard methods, mounted in immersion oil and the number and diameter of vessels at different locations of the vascular network determined.

RESULTS

A time-sequence series of photographs for the convection of the dye solution in one of the test leaves is presented in Figure 4. Distances of dye penetration along the mid-rib and in the branches were recorded on film as functions of time. As the dye solution flowed in the xylem vessels, the dye diffused into the cell walls of the surrounding tissues with the consequence that the intensity of fluorescence at any location increased with time. The tip of the fluorescence in each vein defined, however, the distance of dye penetration. Both lateral diffusion of the dye into the surrounding tissues and axial dispersion of the dye in the vessel bundles (diffusion superposed on bulk flow) were estimated to occur at rates slow compared to the bulk flow in the open channels of the vessels. It was assumed for the calculations that the average velocity of flow in the individual vessels were the same for all vessels at any particular vein cross-section such that the flow into any branch is determined by the number and dimensions of vessels in the traces. This assumption is equivalent to modelling the flow as though the fluid was percolating through a highly anisotropic porous medium in a vein. This is reasonable since many vessels were juxtaposed, laterally connected through pits (microscopic pores), and were congregated within the bundles.

The total cross-sectional area of vessels as a function of axial distance along the mid-rib and along branches (from junction with the previous generation) are presented in Table 1 for a test leaf sample. The population of vessels and the cross-sectional areas available for flow exhibit overall decreasing trends along a vein. The decreases were, however, not monotonic. Upstream of a junction where a trace apparently diverged, the cross-sectional flow area increased. An examination of sections of fresh leaves revealed that the vascular bundle traces which entered vein branches had separated from the principal bundle a distance ahead of the apparent junction. This is obvious from some of the photographs in Figure 4 (divergence from the mid-rib). A few of the first generation branches even had traces already distinctly separated in the petiole of the leaf.

Velocity calculated from the slope of the distance-time data was multiplied by vessel cross-sectional area at a point to establish the local bulk flow rate. Flow cross-sectional areas at any location must be carefully defined since bundles separated from the major bundle were subject to different force fields downstream and might exhibit velocities different from that of the main bundle even before the apparent junction. An assumption inherent in the analysis was that the leaf transpiration rate (at all sites) was steady for the duration of the experiment of between 2 and 5 minutes depending on the relative humidity of the room air. That is, different parts of the leaf should not be adjusting their rates of water flow within the experimental period even if the overall rate of water uptake remained constant. Typical volumetric flow rate results for the major veins the first generation branches and some minor veins are presented in Figures 5 through 7 for three different leaves.

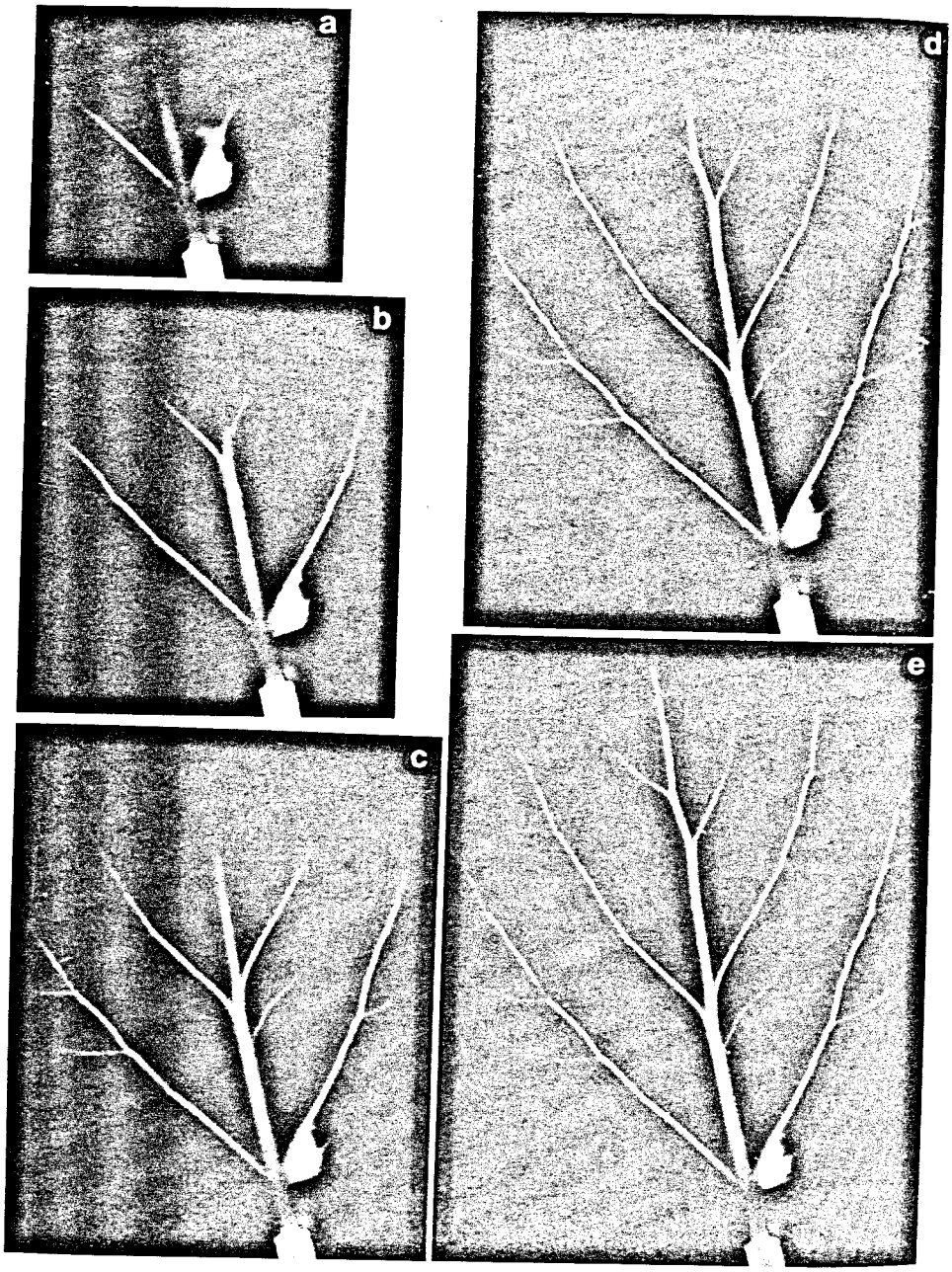

FIG. 4

Images of dye penetration in the leaf vascular network for leaf sample 13 at different times from start of experiment, 2.9X. Room temperature = 19.4°C, relative humidity = 82.5% (a) 48s, (b) 73s, (c) 103s, (d) 143s, (e) 176s. Divergence of traces are visible in (d) and (e).

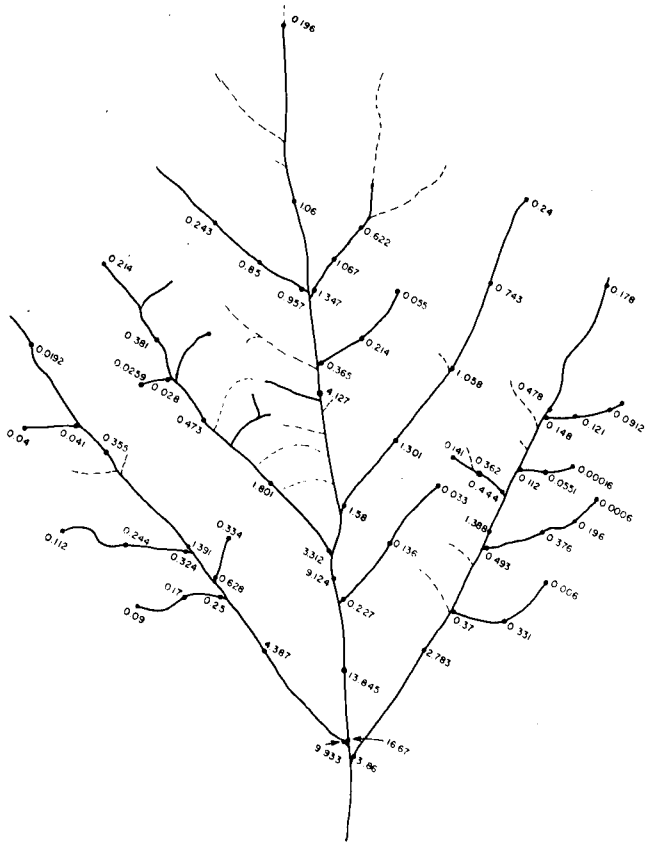

FIG. 5

Local flow rates x 10^{-5}, $\mu m^3/s$ in leaf sample 13.

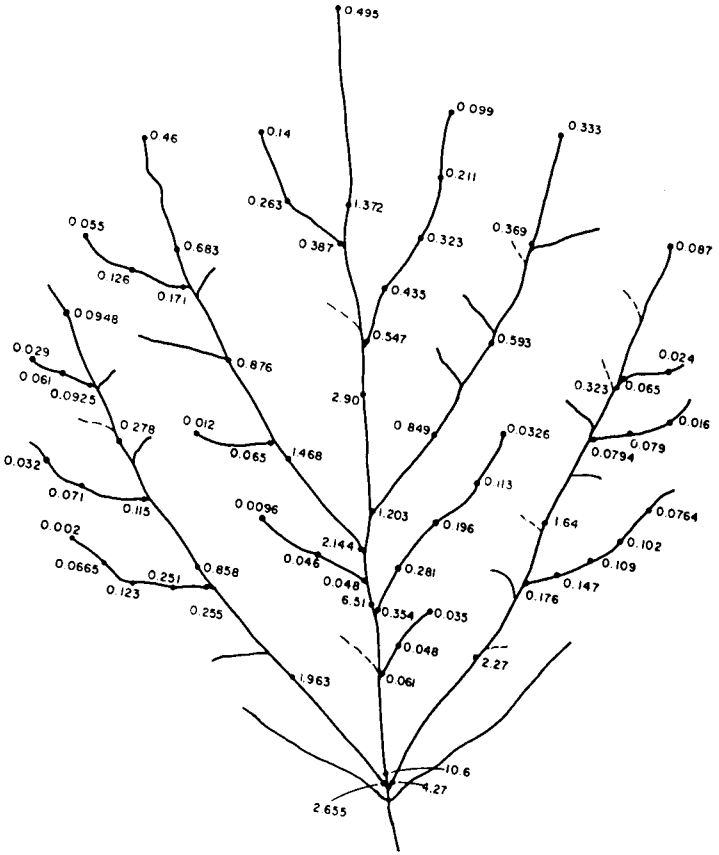

FIG. 6

Local flow rates x 10^{-5}, $\mu m^3/s$ in leaf sample 17.

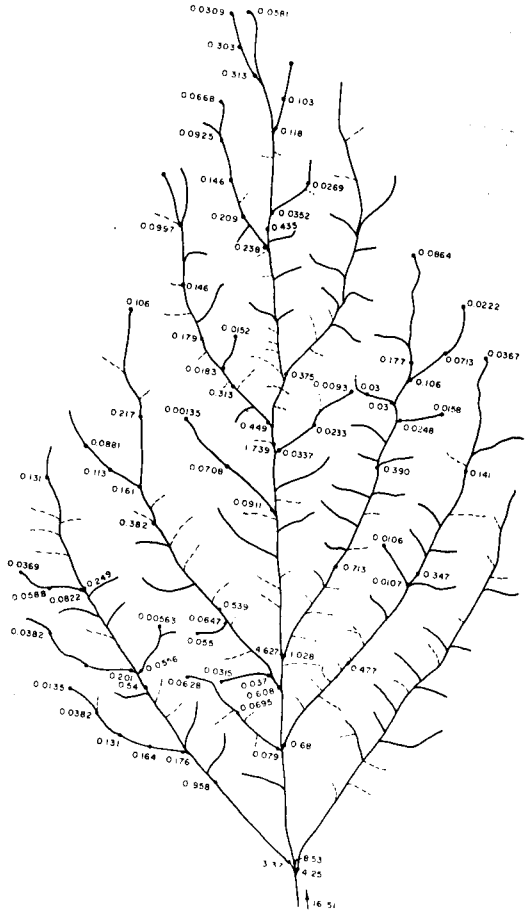

FIG. 7

Local flow rates x 10^{-5}, $\mu m^3/s$ in leaf sample 22.

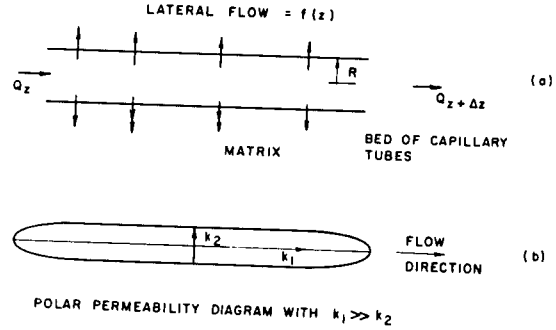

POLAR PERMEABILITY DIAGRAM WITH $k_1 \gg k_2$

FIG. 8

(a) Model of a vascular bundle

(b) Polar permeabilities (not to scale)

An Analysis for the Local Pressures in the Veins

For the leaves investigated, the xylem vessel diameters were between 3.5 and 13 μm and their local population varied between 3 and 76. The collection of tubes in a vein was modelled as a highly anisotropic porous medium with axially-directed permeabilities much greater than the lateral values. This is illustrated in Figure 8.

At steady-state, the continuity equation for a differential segment of a vein is

$$\frac{\partial(q_z A_z)}{\partial z} = -\,2\pi R q_r\Big|_{r=R} \tag{1}$$

where q_z and q_r are the mass fluxes in the axial and radial directions respectively, R is the effective radius of a bundle and A_z is the local sum cross-sectional areas of the vessels. The fluxes are obtained from Darcy's equation. That is:

$$q_z = -\frac{k_1}{\mu}\frac{\partial P}{\partial z} \quad \text{and} \quad q_r = -\frac{k_2}{\mu}\frac{\partial P}{\partial r} \tag{2}$$

where k_1, k_2 are the directional permeabilities and μ is the liquid viscosity. Since q_z, q_r A_z, k_1 and k_2 may vary with axial position along a vein, equation (1) may be re-stated as

$$-\frac{A_z}{\mu}\left\{\frac{\partial P}{\partial z}\cdot\frac{\partial k_1}{\partial z} + k_1\frac{\partial^2 P}{\partial z^2}\right\} - \frac{k_1}{\mu}\frac{\partial P}{\partial z}\frac{\partial A_z}{\partial z} = 2\pi R\left(\frac{k_2}{\mu}\frac{\partial P}{\partial r}\right)\Big|_{r=R} \tag{3}$$

Equation (3) simplifies to

$$\left(\frac{k_1 A_z}{\mu}\right)\frac{\partial^2 P}{\partial z^2} + \left(\frac{A_z}{\mu}\frac{\partial k_1}{\partial z} + \frac{k_1}{\mu}\frac{\partial A_z}{\partial z}\right)\frac{\partial P}{\partial z} + \left(\frac{2\pi R}{\mu}\right)\left(k_2\frac{\partial P}{\partial r}\right)\Big|_R = 0 \tag{4}$$

The last term on the left of the equal sign is the lateral flow rate from the bundle. This term is a function of z and is evaluated from experimental data since both terms in the bracket cannot be readily determined separately.

If the tubes were straight, smooth walled and non-porous, the permeability in the axial direction, k_1, would be given by (10),

$$k_1 = \varepsilon\frac{\bar{\delta^2}}{32} \tag{5}$$

where $\bar{\delta^2}$ is the average of the squares of the diameter of the vessels and ε is the media porosity. For contiguous tubes, ε approaches unity. Because the capillary tubes are internally sculptured (secondary deposits of cellulose as rings, helices or simple intussusceptions (11,12)), have porous walls and finite lengths (13), k_1 is not as simply represented as in equation 5. For the present, k_1 will be represented by

$$k_1 = \frac{\chi\bar{\delta^2}}{32} = \frac{\chi A_z}{8\pi n} \tag{6}$$

where χ is an empirical correction factor which may be position dependent and n is the number of tubes in the veins at the location of interest. For the moment, χ will be assumed, for lack of pertinent data, to be a constant.

When equation (6) is substituted into equation (4) and the equation is re-arranged, a non-homogeneous second order, ordinary differential equation results. That is:

$$\frac{d^2P}{dz^2} + \left(\frac{2}{A_z}\frac{dA_z}{dz} - \frac{1}{n}\frac{dn}{dz}\right)\frac{dP}{dz} + \frac{Z(z)}{Y}\cdot\frac{n}{A_z^2} = 0 \qquad (7)$$

where $$Z(z) = \frac{2\pi Rk_2}{\mu}\frac{\partial P}{\partial z}\Big|_R = \frac{\partial Q}{\partial z} \quad \text{(rate of lateral withdrawal)} \qquad (8)$$

and $$Y = \frac{\chi}{8\pi\mu}$$

Equation (7) may be re-written as

$$\frac{d^2P}{dz^2} + \left(\frac{\partial \ln \bar{\delta}^2}{\partial z} + \frac{\partial \ln A_z}{\partial z}\right)\frac{dP}{dz} + \frac{Z(z)}{A_z\bar{\delta}^2}\frac{\pi}{4} = 0 \qquad (9)$$

With the boundary condition that at the junction of the leaf lamina and the petiole, and at the branch insertions, $dp/dz \sim 0$ because vessel areas at these points are locally increased substantially in anticipation of branching, equation 9 can be integrated once by the integrating factor method to yield

$$\frac{dP}{dz} = \frac{32\mu}{A_z\bar{\delta}^2}\left\{Q(0)\left(\frac{1}{\chi} - 1\right) - \frac{Q(z)}{\chi}\right\} \qquad (10)$$

For a first approximation, $\chi \sim 1$ and the pressure gradient at z is given by

$$\frac{dP}{dz} = -\frac{32\mu}{A_z\bar{\delta}^2}Q(z) \qquad (11)$$

where $Q(z)$, A_z and $\bar{\delta}^2$ at z are evaluated from experimental data. The pressure at z could then be determined from

$$P = \int_{z=0}^{z}\left(\frac{dP}{dz}\right)dz + P_o \qquad (12)$$

From studies on creeping flows in corrugated tubes (14), χ has been found to be between 1.1 and 1.4 depending upon the degree of wall roughness and flow rates. That is, k_1 in equation 6 is actually larger than values for fully developed Poiseuille's flow in a smooth straight tube of similar diameters. The continuity of flow through axially contiguous vessels is, however, maintained by the water passing through pits which would substantially increase the drag. This is similar to water passing through sieve plates at periodic intervals in a pipe. The ultimate χ is suggested to be close to unity (15,16). Other non-darcian effects such as ionic interactions between the low concentration ions in the xylem sap and the charged cellulosic walls (17) may also be important.

The pressures calculated from equations 11 and 12 at various locations in the vascular network of the test leaves (Figures 5-7) are presented in Figures 9 through 11. The reference point has been arbitrarily chosen as

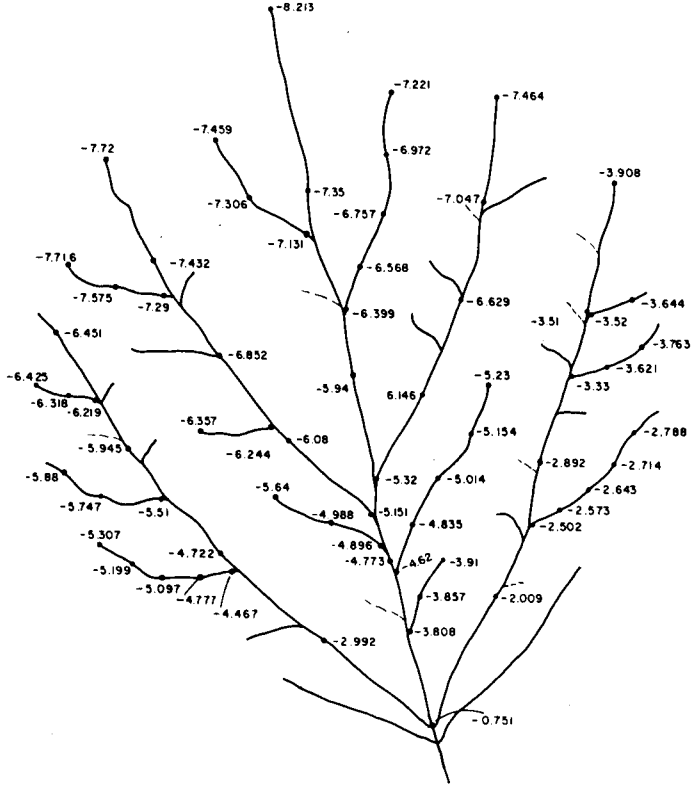

FIG. 9

Local relative pressures, kPa, at different sites in the vascular network for leaf 13.

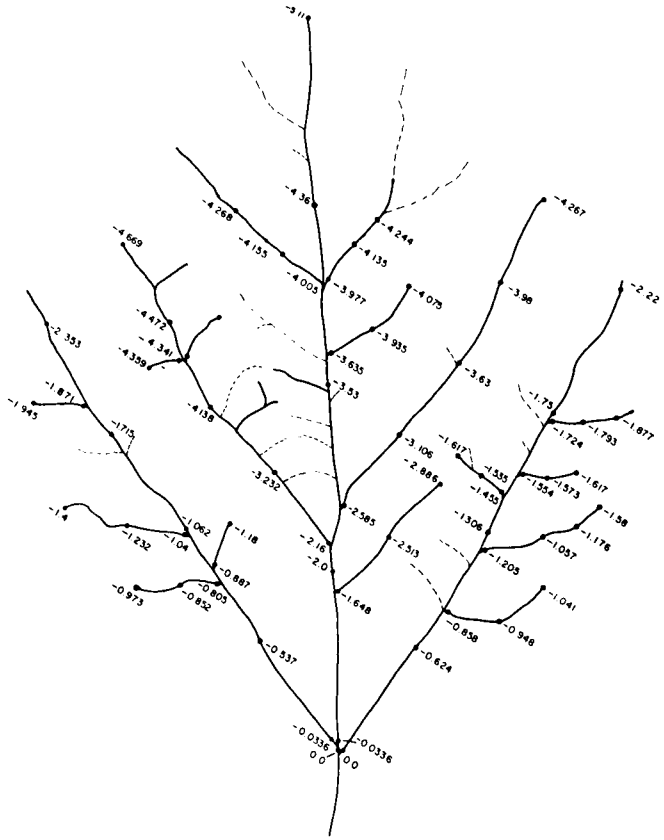

FIG. 10

Local relative pressures, kPa, at different sites in the vascular network for leaf 17.

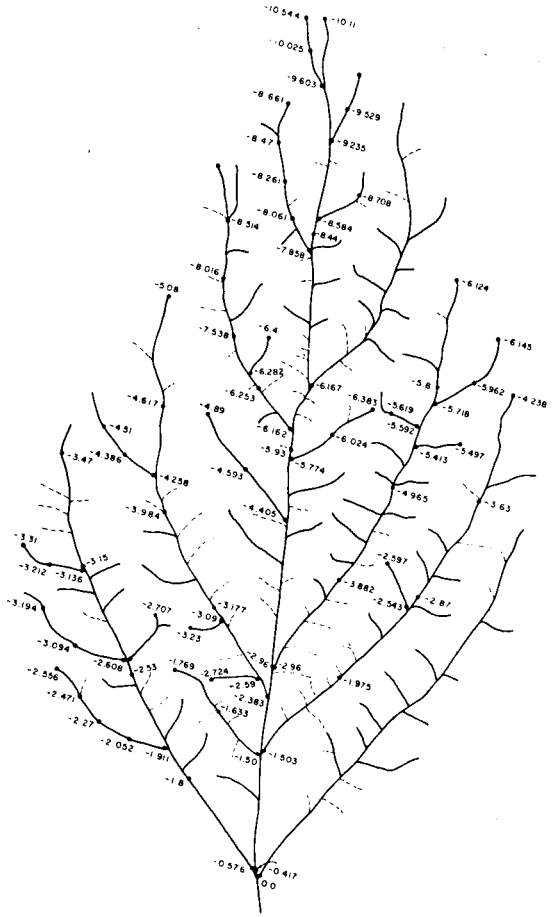

FIG. 11

Local relative pressures, kPa, at different sites in the vascular network for leaf 22.

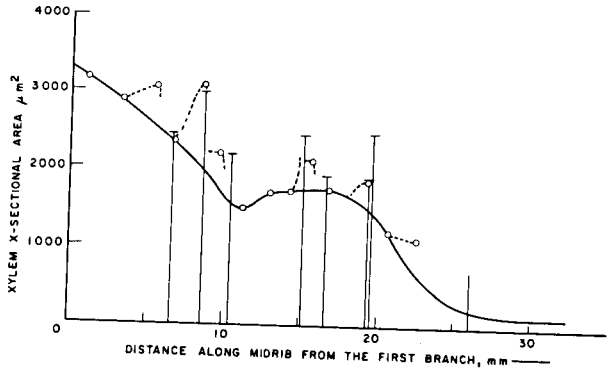

FIG. 12

Overall conduit cross-sectional areas along the mid-rib of leaf 17 from the first branch junction. The solid line represents non-diverging vessels. Dashed lines show areas including branch traces. Bars show the location and total vessel areas after a junction.

the junction of the first branch and the leaf mid-rib. For the detached leaves, this base pressure would not be significantly different from atmospheric pressure. On the tree, the reference pressure would be quite different and would depend upon the location of leaf attachment to the plant, the transpiration rates and external conditions, and the xylem tension at the point of leaf insertion. The pressures also reflect those in the tracheal elements, not those in the apoplast of the cell walls through which the water must percolate for its ultimate evaporation.

DISCUSSIONS

As is evident in Figures 5 through 7, the water that enters the leaf via the petiole is very rapidly dispersed laterally out of the tracheal elements into the surrounding matrix of cell walls. In Table 2, the percentage of inlet water withdrawn from the tracheal elements into the surrounding tissues at different radial distances from the first branch of

TABLE 2

Percent of inlet water transferred out of veins within radial distances 0.25L, 0.5L and 0.75 L from 1st branch off the mid-rib. (L=length of mid-rib).

Test Leaf	Temp. °C	Relative Humidity %	Length of mid-rib, L cm	Flow Rate at base of lamina x 10^{-5} $\mu m^3/s$	% of Inlet Flow Withdrawn 0.25L	0.5L	0.75L
13	19.44	82.5	3.107	17.53	38.9	64.7	81.9
17	19.44	82.5	3.09	30.46	49.9	76.8	92.2
22	19.83	82.5	4.457	16.15	55.7	82.2	94.6

the mid-rib are presented. For the three leaves, within 25% radius of the mid-rib length, between 38.9 and 55.7% of the feed water had been transferred out of the tracheal elements. For sample 13, the sum of the lengths of mid-rib and first two generation veins within this region corresponds to 40.1 mm. In the entire leaf, the total length of veins was 218.3 mm, i.e. ~ 18.4% of the total major veins length was involved in dispersing 38.9% of the feed water in this region. The length of the vessels, consequently, is not correlated to the withdrawal rate as implied by Wylie (5). Within 50% of the radius of the mid-rib, between 64.7 and 82.2% of the inlet water has been withdrawn. Between 81.9 and 94.6% of the water has left the tracheal elements in the radius of 0.75 L. Since each leaf lamina is effectively compartmentalized by the bundle sheaths on minor veins, the data indicates that most of the inlet water is transpired at the base of the leaf. This is consistent with observations that, when a plant is subjected to a gradual water stress such as in a drought condition, the apical parts of the leaves wilt first. Leaf sample 13 was younger than the other two leaves and this may account for the lower values of water dispersion at the laminar base. Cells close to the apex might still be in the rapid growth phase and the local tension drawing the water could be higher than at a later stage.

The foregoing results may have important ramifications for the temperature regulation of the leaf and how transpiration data are analyzed.

A disproportionate evaporation of water in the basal part of a leaf would appear to imply that this area should be cooler than near the apex during active transpiration. This may, however, not be true. The leaf blade is generally thicker as well at the leaf base and the internal area for evaporation and the volume of cells enclosed by the epidermis may be substantially larger than for the same projected leaf surface area closer to the apex. Observable temperature differences would therefore be minimized. Furthermore, stomatal aperture sizes and stomata population in an area would not be simply related to the capacity for transpiration within a leaf surface area. That is, the mechanical facilities for regulating transpiration rates does not alone define how fast the process occurs. The internal geometric and chemical characteristics of the leaf mesophyll would be important (18).

From the flow patterns, it is obvious that the flow in the first two branches off the mid-rib accounts for a substantial portion of the inlet stream. As noted earlier, these branches have their own traces (or vascular bundles) in the petiole. The more distal first generation branches typically have traces derived from the principal bundle of the mid-rib. These traces are distinctly visible in the mid-rib cross-section as shown in Figure 4 and the connection may be a few millimeters upstream of the externally visible branch junction. The connection region can generally be determined from the pattern of total vessel cross-sectional areas along a vein. Where a branch trace is formed, the flow area typically increases gradually and there is almost a discontinuous decrease along the axis when the branch trace emerges into its own vein. This is illustrated in Figure 12 where the solid curve is a plot of the vessel cross-sectional area that convects water axially along the mid-rib. The dashed curves show the total cross-sectional area of all vessels at any point along the mid-rib, that is, the combined branch traces and principal trace vessel areas. The bars show the location and areas for the vessels emerging from a branch junction.

For most branches, the measured vessel areas at the base were higher than at the other locations downstream. That is, there was no evidence of area contraction at the departure of a trace. However, the diameters of vessels entering the trace were consistently smaller than in the axial bundle. The hydraulic bottleneck at branch junctions described by Zimmermann (19) may, consequently, be reflected by the increased friction in narrower vessels.

The pressure distributions in Figures 9 through 11, as noted earlier are relative to the first vein branch junction. The pressure drops along the mid-ribs are seen to be specific to a leaf. For the three samples, the overall pressure gradients (base to tip along the mid-rib) were between -1.63 and -2.61 atm/m. The pressure gradients were, however, not constant along a mid-rib or a branch. Maximum absolute gradients were typically observed a short distance after a branch trace emerged from the previous generation. These overall values are considerably higher than ~ 0.1 atm/m for flow in xylem vessels as estimated from the Hagen-Poiseuille equation (20).

It is important to note that the pressure drop along vessels should be considerably smaller than required to transport water from the tracheal elements to the sites of evaporation. In the cell walls, water must permeate a force space of cellulosic strands embedded in hemicelluloses, lignin and other polymeric substances (12). The parenchyma cell walls are themselves very thin, in the order of 0.1 μm (21) and cellular arrangements are such that contiguous cells only touch in small areas. From the results, it may also be deduced that the tension (negative pressure) within an areole close to the leaf base would not be considerably different from

that of an areole close to the leaf apex. This would imply that there are no special differentiation of the cell wall thicknesses and imbibition characteristics. If the actuating forces for water percolation are of the same order of magnitude, the areole close to the base would be able to withdraw more water from the neighbouring tracheal elements which have both larger surface areas for lateral dispersion and a greater volume of water throughput from which to extract.

ACKNOWLEDGEMENTS

Yuen Chow's expert technical assistance in the execution of the experiments is much appreciated. The work was supported by a grant from the Natural Science and Engineering Research Council of Canada. The study is humbly dedicated to the memory of Martin Huldrych Zimmermann (Harvard University).

REFERENCES

1. STRUGGER, S. Die Erforschung des Wasser - und Nahrsalztransportes im Pflanzenkorper mit Hilfe der fluoreszenzmikroskopischen Kinomatographie. Arbeitsgemeinsh. f. Forschung d.Landes Nordrhein - Westfahlen. Heft 21a. Westdeutscher Verlag Koln und Opladen, 1953.

2. STRUGGER, S. Faszikulare und extrafaszikulare Wasserleitung. Institute fur Film und Bild in Wissenschaft und Unterbricht. Hochschulfim C 601/1950.

3. ESAU, K. Plant Anatomy. (2nd ed.) John Wiley, New York. 1965, ch. 16.

4. WYLIE, R.B. Conduction in dicotyledon leaves. Iowa Acad. Sci. Proc. 53, 195-202, 1947.

5. WYLIE, R.B. The bundle sheath extension in leaves of dicotyledons. Am. J. Bot. 39, 645-51, 1952.

6. STRAIN, R.W. A study of vein endings in leaves. Amer. Midland Nat. 14, 367-375, 1933.

7. WYLIE, R.B. Relations between tissue organization and vein distribution in dicotyledon leaves. Amer. J. Bot. 26, 219-225, 1939.

8. ARMACOST, R. R. The structure and function of the border parenchyma and vein-ribs of certain dicotyledon leaves. Iowa Acad. Sci. Proc. 51, 157-169, 1945.

9. WYLIE, R.B. The role of the epidermis in foliar organization and its relations to the minor venation. Amer. J. Bot. 30, 273-280, 1943.

10. SCHEIDEGGER, A.E. The Physics of flow through porous media. Univ. of Toronto Press, p115-117, 1960.

11. OHTANI, J. and ISHIDA, S. An observation of the sculptures of the vessel wall of Fagas crenata BL. using scanning electron microscopy. Res. Bull. College Expt. For., Hokkaido Univ. 30, 125-144, 1973.

12. FREY-WYSSLING, A. The Plant Cell Wall. Gebruder Borntraeger. Berlin, 1976.

13. ZIMMERMANN, M.H. and JEJE, A. Vessel-length distribution in stems of some American woody plants. Can. J. Bot. 59, 1882-1892, 1981.

14 JEJE, A. Flow Structures in living plant microcapillaries. Submitted for review. 1984.

15. BERGER, W. Das Wasserleitungssystem von krautigen Pflanzen, zwergstrauchern und lianen in quantitativer Betrachtung. Beih. Bot. Cbl. 48(I), 363-390, 1931.

16. MUNCH, E. Durchlassigkeit der Siebrochen fur Druckstromungen. Flora 136, 223-262, 1943.

17. TYREE, M.T. and ZIMMERMANN, M.H. The theory and practice of measuring transport coefficients and sap flow in the xylem of red maple stems (Acer rubrum). J. Expt. Bot. 22, 1-18, 1971.

18. THOMAS, M., RANSON, S.L. and RICHARDSON, J.A. Plant Physiology, 5th ed. Longman, London, pp. 311-317, 1973.

19. ZIMMERMANN, M.H. Xylem structure and the ascent of sap. Springer-Verlag, Berlin. 1983.

20. ZIMMERMANN, M.H. and BROWN, C.L. Trees: Structure and Function. Springer-Verlag, Berlin. 1971.

21. LEDBETTER, M.C. and PORTER, K.R. Introduction to the fine structure of Plant Cells. Springer-Verlag, New York. 1970.